ACS APPLIED MATERIALS & INTERFACES

RESEARCH ARTICLE

www.acsami.org

Graphene/Silicon Nanowire Schottky Junction for Enhanced Light Harvesting

Guifeng Fan, Hongwei Zhu,* Kunlin Wang, Jinquan Wei, Xinming Li, Qinke Shu, Ning Guo, and Dehai Wu

Key Laboratory for Advanced Manufacturing by Material Processing Technology, Ministry of Education and Department of Mechanical Engineering, Tsinghua University, Beijing 100084, P. R. China

Supporting Information

ABSTRACT: Schottky junction solar cells are assembled by directly coating graphene films on n-type silicon nanowire (SiNW) arrays. The graphene/SiNW junction shows enhanced light trapping and faster carrier transport compared to the graphene/planar Si structure. With chemical doping, the SiNW-based solar cells showed energy conversion efficiencies of up to 2.86% at AM1.5 condition, opening a possibility of using graphene/semiconductor nanostructures in photovoltaic application.

KEYWORDS: graphene, silicon nanowires, Schottky junctions, solar cells

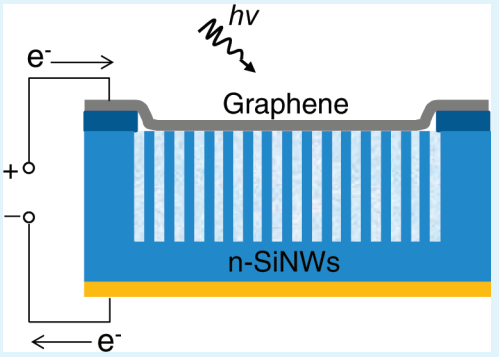

INTRODUCTION

Graphene,[1] a two-dimensional single atomic layer of crystalline carbon, is featured with its unique Dirac electronic band-structure, high room-temperature carrier mobility of 15000 $cm^2 V^{-1} s^{-1}$[2] and Fermi velocity of 1×10^6 m/s,[3] tunable band gap,[4] the ballistic transport with a mean-free path of 300−500 nm,[5] and visible transparency of 97.7%.[6] The structural flatness makes graphene a near-ideal flat surface for conformal assembly toward device integration. Especially, graphene has shown great potential for creating photovoltaic solar devices owing to its high optical transmittance, electrical conductivity, and surface area.[7,8] There have been several attempts to incorporate graphene into various solar cells as transparent electrodes,[9−15] electron acceptors,[16−21] hole collectors,[22] counter electrodes,[23,24] photoactive promoters.[25−27] Recently, we reported the first demonstration of graphene/n-type silicon (G/Si) Schottky junction solar cells.[28] As illustrated in Figure 1a, the graphene film not only serves as a transparent electrode for light transmission, but also an active layer for electron/hole separation and hole transport. Meanwhile, graphene acts as an antireflection coating which reduces reflection by ∼70% in the visible region and ∼80% in the near-IR region. The G/Si solar cells showed power conversion efficiencies (η) up to 1.6% at air mass 1.5 (AM1.5, 100 mW/cm^2) condition. In light of this work, carbon-based hybrid thin films, consisting of agglomerated graphene nanowhiskers embedded in a uniform matrix of amorphous carbon, were also prepared via a pyridine chemical vapor deposition (CVD) method.[29] Schottky solar cells made from the hybrid films and n-Si showed η of ∼1% under AM1.5 illumination. Furthermore, freestanding carbon-based composite thin films of carbon nanotube (CNT) and graphene, were assembled by a solid-phase layer-stacking approach.[30] Under AM1.5 illumination, heterojunction solar cells made from the composite films and n-Si showed maximum η of 5.2%.

The efficiency of the G/Si cells could be further increased with improvements in graphene quality, interface optimization and appropriate use of the photoactive semiconductors. Nanostructured semiconductors are expected provide not only a large interface area for light trapping but also fast electron transport in semiconductors. For example, photovoltaic cells based on silicon nanowire (SiNW) arrays have emerged as a promising candidate for solar energy harvesting.[31−34] Though traditional planar bulk-form p-n junction devices currently still dominate the field of commercial photovoltaic power, the unique optical and electronic properties of SiNWs make them more suitable for next-generation photovoltaic applications. SiNW arrays with moderate filling ratio have much lower reflectance compared to thin films in a wide spectrum range, which can be achieved without specially designed antireflection coatings.[35,36] Each individual nanowire in the array forms a p-n junction in nanoscale and acts as a photovoltaic microcell. In the radial (core−shell) nanowire structure, photoexcited electrons and holes travel very short distances before being collected by the electrodes, resulting in higher charge-collection efficiencies,[37−41] and this advantage

Received: October 25, 2010
Accepted: January 31, 2011
Published: February 16, 2011

leads to a higher tolerance for material defects. In the last years, SiNW-based photoelectrochemical solar cells have been subject of intensive research to facilitate light absorption and radial collection of photogenerated carriers.[42−45]

RESULTS AND DISSCUSION

Considering the application potential of SiNWs, in this paper we are aiming to further increase the G/Si cell efficiency by using SiNWs instead of planar silicon. We deposited graphene films on vertically aligned n-type SiNWs to make Schottky junctions (Figure 1b). The advantages of using SiNWs are: (i) to provide more surface area for light harvesting, (ii) to suppress light reflection; (iii) to reduce the use of silicon materials. Figure 1c shows a comparison of the reflection spectra of planar Si, SiNWs, G/Si, and G/SiNWs. It is clear that the SiNWs impart a significant reduction of the reflectance compared to the bulk silicon. When combined with graphene, the G/SiNW junction shows relatively high optical absorption comparing to the G/Si structure.

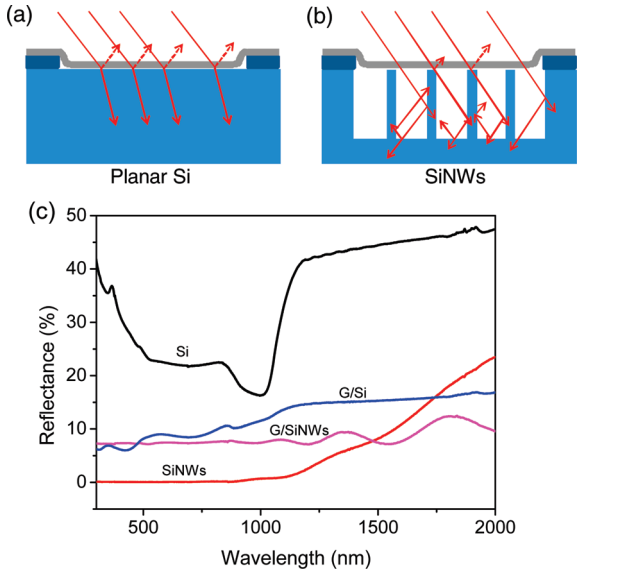

Figure 1. Schematics of (a) G/planar Si and (b) G/SiNW junctions. (c) Reflection spectra of planar Si, SiNWs, G/Si, and G/SiNWs.

The device schematic of the G/SiNW solar cell is shown in Figure 2a. Graphene films were synthesized by a methane CVD method using nickel foils as substrates.[28] Freestanding graphene films were obtained by detaching the films from the nickel substrate in a $HCl/FeCl_3$ mixture solution, followed by rinsing with deionized water. It is worth mentioning the graphene film grown on Ni foil consists of multiple layers of overlapped graphene sheets which provide balanced conductivity and transparency. SiNW arrays were prepared from n-type (100) silicon wafers by a silver-assisted etching method and then treated in a HF and HNO_3 aqueous solution.[31] As-prepared SiNW samples were cut into plates of 1.2 × 1.2 cm^2. A piece of insulating tape with a circular hole (6 mm in diameter) was adhered on the top of the SiNW array. The back electrode was made using sputtered Ti/Pd/Ag on the bottom of the silicon wafer to achieve a good ohmic contact. Graphene was then transferred directly to the top of the SiNW array to make a junction.

Microstructure of SiNW arrays was investigated by scanning electron microscope (SEM). Figure 2b shows the top-view SEM image of a typical SiNW array, in which nanowires are uniformly distributed. The area density of the SiNWs is about ~5 × 10^8/mm^2. The inset shows the cross-sectional view of the vertically aligned SiNW array with a height of ~1.8 μm. It is worthy to mention that for SiNWs, the large length/diameter ratio will result in considerable diffuse reflectance losses.[36] This height value was chosen based on our previous study which revealed that the SiNW array of ~2 μm high showed the best photovoltaic performance.[46] Figure 2c shows the top-view SEM images of the G/SiNW junction, demonstrating a conformal coating of the

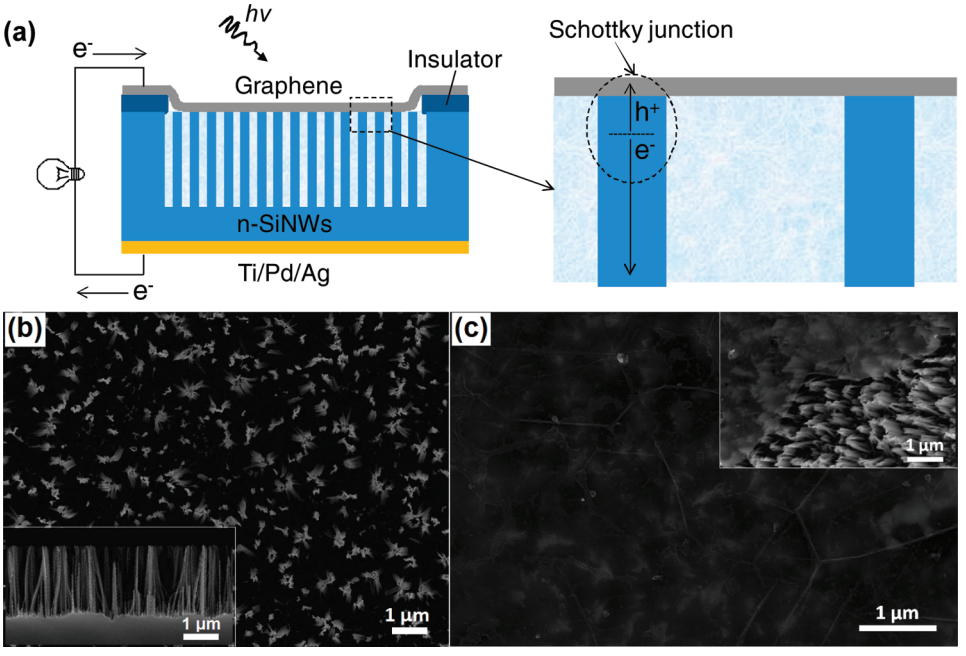

Figure 2. (a) Schematic of the G/SiNW solar cell. (b) Top-view and side-view (inset) SEM images of SiNW array. (c) Top-view SEM images of G/SiNW junction.

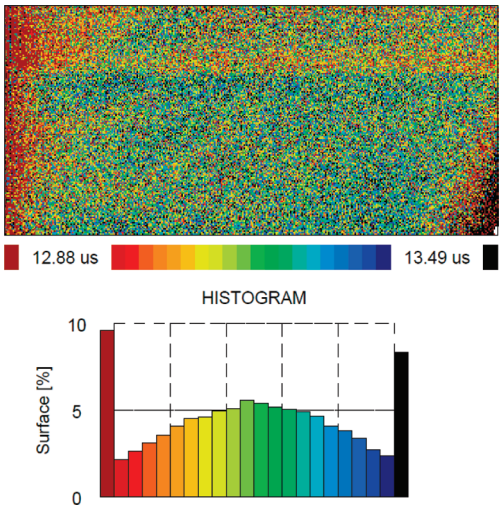

Figure 3. Minority carrier lifetime map and distribution of a SiNW array.

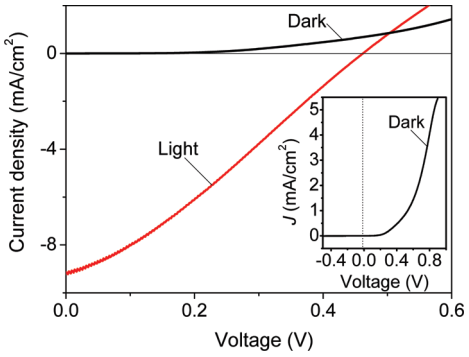

Figure 4. Dark and light $J-V$ curves of a G/SiNW solar cell.

semitransparent graphene film on the SiNW array. As shown in the inset of Figure 2c, the underlying SiNWs can be clearly observed at a place where graphene was intentionally removed.

The G/SiNW structure consists of $\sim 9 \times 10^8$ Schottky junction microcells. As shown in the right panel of Figure 2a, each microcell is composed of two key components: graphene and a single SiNW. Graphene acts as a seamless transparent electrode that is favorable for collection and transport of the photoexcited holes generated in the SiNW.

The minority carrier lifetime of the SiNW array was measured by microwave photoconductive decay (μ-PCD) technique via a WT-2000 system (Semilab Inc.). High resolution minority lifetime map (Figure 3) of a typical 2×1 cm^2 SiNW array shows a uniform lifetime distribution. From the figure, one can distinguish the uniformity of the array by different color distributions (bottom panel) which represent the minority-carrier lifetime. Most of the lifetimes distribute from 12.8 to 13.5 μs. The average lifetime is $\sim$13.2 μs, which is much higher than the reported values ($\sim$15 ns) for CVD grown SiNWs.[48] Our calculation also indicated that the SiNWs have a large minority carrier diffusion length (L) of $\sim$130 μm by using the equations

$$L = (D\tau)^{1/2} \text{ and } D = kT\mu/q$$

where τ is the lifetime, D is the diffusion coefficient, k is the Boltzmann constant, T is absolute temperature, μ is the mobility (the doping level of our SiNWs is $\sim 2 \times 10^{15}$ cm^{-3}, which corresponds to a mobility of $\sim 5 \times 10^2$ cm^2/(V s)),[47] and q is electronic charge.

The G/SiNW solar devices were tested with a Newport solar simulator under AM1.5 condition at 100 mW/cm^2. The current−voltage data were recorded using a Keithley 2601 SourceMeter. Forward bias is defined as positive voltage applied to the graphene film. Dark current density−voltage ($J-V$) curves obtained from the G/SiNW cells exhibit rectifying characteristics (one example is shown in the inset of Figure 4), and demonstrate that the G/SiNW heterostructures behave as well-defined diodes. The nonlinear $J-V$ characteristic of the Schottky junction can be expressed by the thermoionic emission model[47]

$$J = J_s\left[\exp\left(\frac{-qV}{nkT}\right) - 1\right]$$

where J_s is the reversed saturated current density and n is the diode ideality factor, which can be estimated as 2−5.5 through curving fitting.

Upon illumination, the G/SiNW devices displayed fairly good photovoltaic response. As shown in Figure 4, light $J-V$ data of a typical G/SiNWs cell shows down-shift curve with an open-circuit voltage (V_{oc}) of 0.462 V, a short-circuit current density (J_{sc}) of 9.2 mA/cm^2 and a fill factor (FF) of 30%, corresponding to a η of 1.25%. The efficiency is still lower than but comparable to the value (1.6%) of the G/planar Si cell.[28] Considering the sparse structure of the SiNW arrays, the real junction area of G/SiNW structure is only $\sim$20% of that for the G/planar Si configuration. By taking this into account, this value (1.25%) implicates the positive role played by the SiNWs. The enhanced efficiency could be mainly attributed to the following two reasons. First, the SiNWs provide fast and direct pathways to increase the charge carrier collection and transport. Second, the SiNWs can suppress the reflection of the junction surface with improved light harvesting in the visible and near-infrared region.

To further improve the cell performance, we studied a chloride doping method to chemically modify the graphene films. It was found that treatment by thionyl chloride ($SOCl_2$) vapor provided a simple way to significantly increase the efficiencies of the G/SiNW cells (up to 4 folds). Figure 5a shows the dark and light $J-V$ curves of a typical G/SiNW cell before and after $SOCl_2$ treatment. Upon Cl doping, the G/SiNW junction displays a lower turn-on voltage. The η of the cell jumps from 0.68% to 2.86% with the V_{oc} from 0.399 to 0.503 V, J_{sc} from 8.04 to 11.24 mA/cm^2 and FF from 21.2 to 50.6%. We observed that there is no obvious difference in cell performance when the doping time is longer than 100 s (Figure 5b,c). Previous studies have demonstrated in CNT and graphene films that the attachment of Cl using this method led to p-type doping and enhanced sheet conductance.[49−51] Energy-dispersive X-ray spectroscopy (EDX) spectrum confirms that the graphene films were doped by $SOCl_2$ (see Figure S1 in the Supporting Information). Microscopic characterizations (see Figure S2 in the Supporting Information) indicated that fairly good adhesion of functional groups to films was obtained and some wrinkles were eliminated. After 20s treatment, the sheet resistance of the graphene films reached 220 Ω/sq and became stable afterward with a total decrease of $\sim$20% (see Figure S3 in the Supporting Information). Because of these effects, it can be seen that in our experiment exposure to $SOCl_2$ here resulted in a 3-fold decrease in the ideality factor (from 5.6 to $\sim$1.8, see Figure 5d) for the G/SiNW junction. To study its

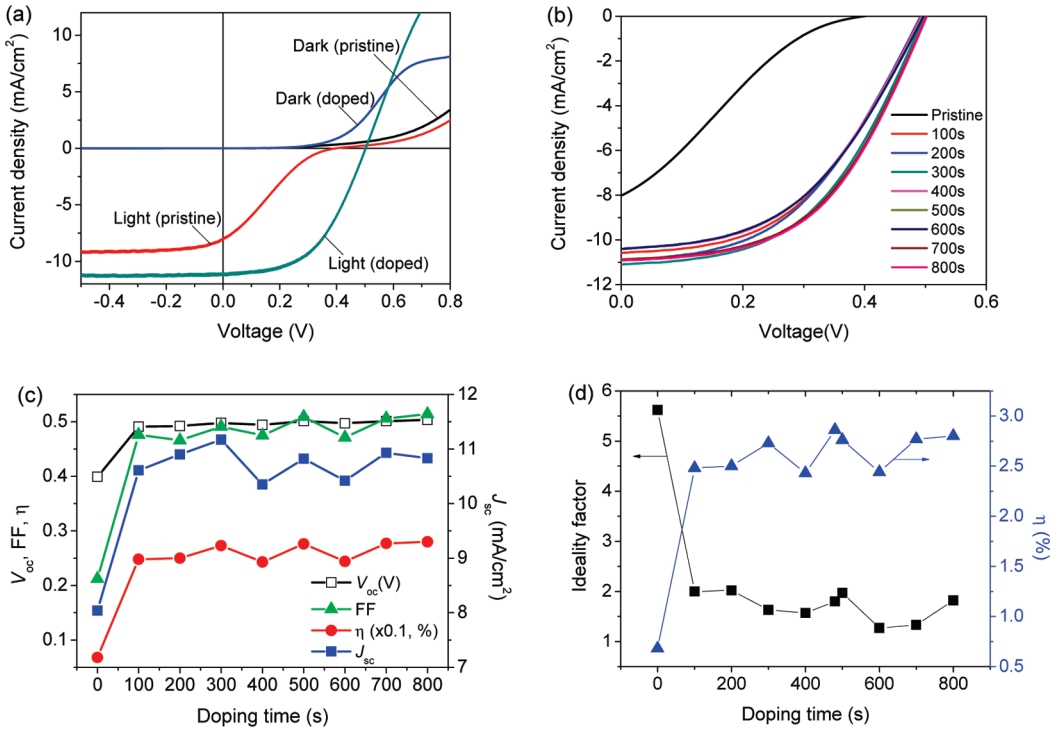

Figure 5. (a) Dark and light $J-V$ curves of a G/SiNW solar cell before and after chemical doping. (b) Light $J-V$ characteristics of different doping time. (c) Plots of V_{oc}, J_{sc}, FF, and η as a function of doping time. (d) Plots of n and η as a function of doping time.

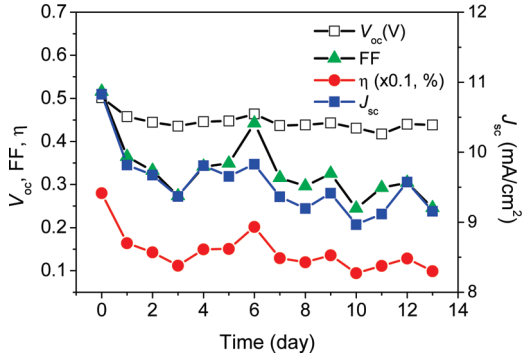

Figure 6. Short-term stability of a doped G/SiNW solar cell.

short-term stability, the cell was then stored in air at room temperature. In the following tests (Figure 6), there is no notable change in V_{oc}. The J_{sc}, FF, and η are gradually decreasing with time except a slight increase on the seventh day and the η is finally stabilized at ~1.2% after 2 weeks.

CONCLUSION

In conclusion, subwavelength diameters and proximity of SiNWs, combined with their micrometer scale lengths, led to interesting optical properties such as low reflectance and high absorption. Schottky junction solar cells based on graphene films and n-type SiNW arrays are demonstrated. Compared to the graphene/planar Si, the graphene-on-SiNW structure shows enhanced light trapping and faster carrier transport. With chemical doping, the SiNW-based solar cells showed energy conversion efficiencies of up to 2.86% under AM1.5 illumination. Our results show that SiNWs are promising materials for photovoltaic application and open a possibility of using graphene/SiNW heterostructures for solar energy harvesting.

METHODS

CVD Synthesis of Graphene. Graphene films were synthesized by a CVD method using nickel foils[28] as substrates. In detail, Ni was gradually heated to 1000 °C in an Ar/H_2 (200/100 mL/min) flow for 1 h. Then methane was introduced with a feeding speed of 20 mL/min in an Ar/H_2 (800/200 mL/min) flow for 10−20 min. Ni was then withdrawn from the heating zone and cooled down to room temperature at a fast cooling rate of 10−20 °C/s. Freestanding graphene films were obtained by etching Ni away in a HCl/$FeCl_3$ solution followed by rinsing with deionized water.

Preparation of SiNW Arrays. SiNW arrays were prepared with Ag-assisted etching method.[31] n-type (100) silicon wafers were cleaned with acetone (5 min) and ethanol (5 min), rinsed with deionized water 2−3 times, then immersed in a 3:1 mixture of H_2SO_4 (97%) and H_2O_2 (30%) for 10 min, thoroughly rinsed with deionized water for 10 min, and then dipped in HF solution for 1 min. The cleaned silicon wafers were immersed into an aqueous HF solution (4.6 M) containing $AgNO_3$ (0.02 M) in an uncovered plastic vessel and treated for 15 min at 50 °C. As-prepared SiNW samples were rinsed in deionized water and dried at room temperature. SiNW arrays were treated in an aqueous solution containing HF (~0.5%) and HNO_3 (~35%) for desired durations, and SiNW array of varied nanowire densities could be obtained.

ASSOCIATED CONTENT

Supporting Information. EDX spectrum, SEM images, and sheet resistance measurement, Figures S1−S3 (PDF). This material is available free of charge via the Internet at http://pubs.acs.org.

AUTHOR INFORMATION

Corresponding Author
*E-mail: hongweizhu@tsinghua.edu.cn.

ACKNOWLEDGMENT

This work was supported by National Science Foundation of China (50972067), Tsinghua National Laboratory for Information Science and Technology (TNList) Cross-discipline Foundation, Foundation for the Author of National Excellent Doctoral Dissertation (201038), and Research Fund for Doctoral Program of Ministry of Education of China (20090002120019).

REFERENCES

(1) Novoselov, K. S.; Geim, A. K.; Morozov, S. V.; Jiang, D.; Zhang, Y.; Dubonos, S. V.; Grigorieva, I. V.; Firsov, A. A. *Science* **2004**, *306*, 666.
(2) Geim, A. K.; Novoselov, K. S. *Nat. Mater.* **2007**, *6*, 183.
(3) Wallace, P. R. *Phys. Rev.* **1947**, *71*, 622.
(4) Han, M. Y.; Özyilmaz, B.; Zhang, Y. B.; Kim, P. *Phys. Rev. Lett.* **2007**, *98*, 206805.
(5) Dragoman, M.; Dragoman, D. *Prog. Quantum Electron.* **2009**, *33*, 165.
(6) Nair, R. R.; Blake, P.; Grigorenko, A. N.; Novoselov, K. S.; Booth, T. J.; Stauber, T.; Peres, N. M. R.; Geim, A. K. *Science* **2008**, *320*, 1308.
(7) Zhu, H. W.; Wei, J. Q.; Wang, K. L.; Wu, D. H. *Sol. Energy Mater. Sol. Cells* **2009**, *93*, 1461.
(8) Hu, Y. H.; Wang, H.; Hu, B. *ChemSusChem* **2010**, *3*, 782.
(9) Wang, X.; Zhi, L. J.; Mullen, K. *Nano Lett.* **2008**, *8*, 323.
(10) Wang, X.; Zhi, L. J.; Tsao, N.; Tomovic, Z.; Li, J.; Mullen, K. *Angew. Chem., Int. Ed.* **2008**, *47*, 2990.
(11) Wu, J. B.; Becerril, H. A.; Bao, Z. N.; Chen, Y. S.; Peumans, P. *Appl. Phys. Lett.* **2008**, *92*, 263302.
(12) Wang, Y.; Chen, X. H.; Zhong, Y. L.; Zhu, F. R.; Loh, K. P. *Appl. Phys. Lett.* **2009**, *95*, 063302.
(13) Zhao, L.; Zhao, L.; Xu, Y. X.; Zhi, L. J.; Shi, G. Q. *Electrochim. Acta* **2009**, *55*, 491.
(14) Arco, L. G.; Zhang, Y.; Schlenker, C. W.; Ryu, K.; Thompson, M. E.; Zhou, C. W. *ACS Nano* **2010**, *4*, 2865.
(15) Xu, Y. F.; Long, G. K.; Huang, L.; Huang, Y.; Wan, X. J.; Ma, Y. F.; Chen, Y. S. *Carbon* **2010**, *48*, 3293.
(16) Liu, Q.; Liu, Z. F.; Zhang, X. Y.; Zhang, N.; Yang, L. Y.; Yin, S. G.; Chen, Y. S. *Appl. Phys. Lett.* **2008**, *92*, 223303.
(17) Liu, Q.; Liu, Z. F.; Zhang, X. Y.; Yang, L. Y.; Zhang, N.; Pan, G. L.; Yin, S. G.; Chen, Y.; Wei, J. *Adv. Funct. Mater.* **2009**, *19*, 894.
(18) Liu, Z. F.; Liu, Q.; Huang, Y.; Ma, Y. F.; Yin, S. G.; Zhang, X. Y.; Sun, W.; Chen, Y. S. *Adv. Mater.* **2008**, *20*, 3924.
(19) Liu, Z. Y.; He, D. W.; Wang, Y. S.; Wu, H. P.; Wang, J. G. *Synth. Met.* **2010**, *160*, 1036.
(20) Liu, Z. Y.; He, D. W.; Wang, Y. S.; Wu, H. P.; Wang, J. G. *Sol. Energy Mater. Sol. Cells* **2010**, *94*, 1196.
(21) Guo, C. X.; Yang, H. B.; Sheng, Z. M.; Lu, Z. S.; Song, Q. L.; Li, C. M. *Angew. Chem., Int. Ed.* **2010**, *49*, 3014.
(22) Eda, G.; Lin, Y. Y.; Miller, S.; Chen, C. W.; Su, W. F.; Chhowalla, M. *Appl. Phys. Lett.* **2008**, *93*, 233502.
(23) Xu, Y.; Bai, H.; Lu, G.; Li, C.; Shi, G. *J. Am. Chem. Soc.* **2008**, *130*, 5856.
(24) Hong, W. J.; Xu, Y. X.; Lu, G. W.; Li, C.; Shi, G. Q. *Electrochem. Commun.* **2008**, *10*, 1555.
(25) Kim, S. R.; Parvez, M. K.; Chhowalla, M. *Chem. Phys. Lett.* **2009**, *483*, 124.
(26) Sun, S.; Gao, L.; Liu, Y. *Appl. Phys. Lett.* **2010**, *96*, 083113.
(27) Yang, N.; Zhai, J.; Wang, D.; Chen, Y.; Jiang, L. *ACS Nano* **2010**, *4*, 887.
(28) Li, X. M.; Zhu, H. W.; Wang, K. L.; Cao, A. Y.; Wei, J. Q.; Li, C. Y.; Jia, Y.; Li, Z.; Li, X.; Wu, D. H. *Adv. Mater.* **2010**, *22*, 2743.
(29) Li, X.; Li, C. Y.; Zhu, H. W.; Wang, K. L.; Wei, J. Q.; Li, X. M.; Xu, E. Y.; Li, Z.; Luo, S.; Lei, Y.; Wu, D. H. *Chem. Commun.* **2010**, *46*, 3502.
(30) Li, C. Y.; Li, Z.; Zhu, H. W.; Wang, K. L.; Wei, J. Q.; Li, X.; Sun, P. Z.; Zhang, H.; Wu, D. H. *J. Phys. Chem. C* **2010**, *114*, 14008.
(31) Peng, K. Q.; Xu, Y.; Wu, Y.; Yan, Y. J.; Lee, S. T.; Zhu, J. *Small* **2005**, *1*, 1062.
(32) Stelzner, T.; Pietsch, M.; Andrae, G.; Falk, F.; Ose, E.; Christiansen, S. H. *Nanotechnol.* **2008**, *19*, 295203.
(33) Gunawan, O.; Guha, S. *Sol. Energy Mater. Sol. Cells* **2009**, *93*, 1388.
(34) Sivakov, V.; Andrae, G.; Gawlik, A.; Berger, A.; Plentz, J.; Falk, F.; Christiansen, S. H. *Nano Lett.* **2009**, *9*, 1549.
(35) Hu, L.; Chen, G. *Nano Lett.* **2007**, *7*, 3249.
(36) Muskens, O. L.; Rivas, J. G. M.; Algra, R. E.; Bakkers, E. P. A. M.; Lagendijk, A. *Nano Lett.* **2008**, *8*, 2638.
(37) Kayes, B. M.; Richardson, C. E.; Lewis, N. S.; Atwater, H. A. *Proceedings of the 31st IEEE Photovoltaic Specialists Conference*; Lake Buena Vista, FL, Jan 3−7, 2005; IEEE: Piscataway, NJ, 2005; p 55.
(38) Garnett, E. C.; Yang, P. D. *J. Am. Chem. Soc.* **2008**, *130*, 9224.
(39) Tian, B. Z.; Zheng, X. L.; Kempa, T. J.; Fang, Y.; Yu, N. F.; Yu, G. H.; Huang, J. L.; Lieber, C. M. *Nature* **2007**, *449*, 885.
(40) Tsakalakos, L.; Balch, J.; Fronheiser, J.; Korevaar, B. A.; Sulima, O.; Rand, J. *Appl. Phys. Lett.* **2007**, *91*, 233117.
(41) Garnett, E.; Yang, P. D. *Nano Lett.* **2010**, *10*, 1082.
(42) Goodey, A. P.; Eichfeld, S. M.; Lew, K. K.; Redwing, J. M.; Mallouk, T. E. *J. Am. Chem. Soc.* **2007**, *129*, 12344.
(43) Maiolo, J. R.; Kayes, B. M.; Filler, M. A.; Putnam, M. C.; Kelzenberg, M. D.; Atwater, H. A.; Lewis, N. S. *J. Am. Chem. Soc.* **2007**, *129*, 12346.
(44) Peng, K. Q.; Wang, X.; Wu, X. L.; Lee, S. T. *Nano Lett.* **2009**, *9*, 3704.
(45) Boettcher, S. W.; Spurgeon, J. M.; Putnam, M. C.; Warren, E. L.; Turner-Evans, D. B.; Kelzenberg, M. D.; Maiolo, J. R.; Atwater, H. A.; Lewis, N. S. *Science* **2010**, *327*, 185.
(46) Shu, Q. K.; Wei, J. Q.; Wang, K. L.; Song, S.; Guo, N.; Jia, Y.; Li, Z.; Xu, Y.; Cao, A. Y.; Zhu, H. W.; Wu, D. H. *Chem. Commun.* **2010**, *46*, 5533.
(47) Sze, S. M.; Ng, K. K. *The Physics of Semiconductor Devices*, 3rd ed.; Wiley Interscience: New York, 2007.
(48) Kelzenberg, M. D.; Turner-Evans, D. B.; Kayes, B. M.; Filler, M. A.; Putnam, M. C.; Lewis, N. S.; Atwater, H. A. *Nano Lett.* **2008**, *8*, 710.
(49) Weglikowska, U. D.; Skakalova, V.; Graupner, R.; Jhang, S. H.; Kim, B. H.; Lee, H. J.; Ley, L.; Park, Y. W.; Berber, S.; Tomanek, D.; Roth, S. *J. Am. Chem. Soc.* **2005**, *127*, 5125.
(50) Eda, G.; Lin, Y. Y.; Miller, S.; Chen, C. W.; Su, W. F.; Chhowalla, M. *Appl. Phys. Lett.* **2008**, *92*, 233305.
(51) Tung, V. C.; Chen, L. M.; Allen, M. J.; Wassei, J. K.; Nelson, K.; Kaner, R. B.; Yang, Y. *Nano Lett.* **2009**, *9*, 1949.